PRESENT STATUS OF THE HIMAC INJECTOR

S. Yamada, T. Hattori,* A. Itano, M. Kanazawa, A. Kitagawa, T. Kohno,
M. Kumada, Y. Miyazawa,† O. Morishita,‡ K. Noda, H. Ogawa, K. Sato,
Y. Sato, K. Sawada,‡ M. Sudou, E. Takada, T. Yamada and Y. Hirao

National Institute of Radiological Sciences
4-9-1 Anagawa, Chiba 260, Japan

Abstract

HIMAC is a heavy ion synchrotron facility dedicated to the medical use especially for the clinical treatment of tumors. The accelerator consists of a 100 MHz injector linac, two separated function type synchrotron rings and a beam delivery system. This paper describes a brief review of a design and present status of the HIMAC injector. Construction of major components of the injector system started in 1987, and will be carried in the HIMAC building early in 1992. The beam tests of the injector will be finished during the fiscal year 1992.

Introduction

The maximum output energy of HIMAC[1] is 800 MeV/u for ions with $q/A = 1/2$. The energy is determined so that the silicon ions can penetrate into a human body with a depth of about 30 cm. The ion species required for the clinical treatment range from ^{4}He to ^{40}Ar. A beam intensity from the HIMAC synchrotron is determined to satisfy the requirements for a dose rate of 5 Gy/min·ℓ in a 14 cm (diameter)×10 cm (depth) irradiation volume. With the dose rate, one irradiation period of heavy ions will be finished within a few minuets.

The injector system of HIMAC comprises a PIG source for light ions, an ECR source for heavier ions, an RFQ linac of 100 MHz and three Alvarez type linac tanks with the same frequency. A debuncher cavity is to be installed in an output beam transport line in order to reduce a momentum spread. The system has no charge stripper either between or before the linac tanks, and will accept heavy ions with a charge-to-mass ratio as small as 1/7. Only one stripper is installed at the end of the Alvarez tank to raise the charge-to-mass ratio to a value higher than 1/4.

Both of the PIG and the ECR sources are installed independently on the high voltage platforms with the maximum voltage of 60 kV. Both sources can be operated with a pulse mode, which is very effective to get high intensity ions with a high charge state especially for the PIG source. The pulse length of the injector beam is longer than 200 μs, because the injection into the synchrotron ring requires an time interval longer than 150 μs for an effective 20 turns.

Since the general descriptions about the HIMAC injector are already given in other articles,[2],[3] only major parameters are described in Table 1.

RFQ and LLBT

An RFQ linac is essentially the same as a 4–vane type RFQ developed at INS.[4] Small changes are made at a diameter of the cavity and a cooling system *etc.* A rather low frequency of 100 MHz is chosen in order to obtain the sufficient focusing strength. A calculated transmission efficiency exceeds 90% for a DC beam with a low focusing strength of $B = 3.8$ which results a high acceleration efficiency. A number of unit cells in the radial matching section is determined to be 40 so that the convergence angle of the input beam becomes as small as 60 mrad.

The RFQ linac is followed by an Alvarez type linac (DTL) operated at the same frequency. The transverse phase space matching between these two type of linacs is accomplished with a quadrupole magnet quadruplet and a horizontal and a vertical steering magnets in an interlinac transport line (LLBT). The LLBT is about 1.9 m long, and some beam diagnostic apparatus of a Faraday cup, an electrostatic pickup electrode, *etc.* are installed in the relatively long transport line.

*Research Laboratory for Nuclear Reactors, Tokyo Institute of Technology, Ohokayama, Meguro-ku, Tokyo 152

†The Institute of Physical and Chemical Research, RIKEN, Hirosawa, Wako-shi, Saitama 351-01

‡Sumitomo Heavy Industries, LTD., Soubiraki-cho, Niihama-shi, Ehime

792

Table 1
Injector specification.

Ion species	^{4}He to ^{40}Ar
Charge to mass ratio	$\geq 1/7$
Ion source type	PIG & ECR
Frequency	100 MHz
Repetition rate	3 Hz Max.
Duty factor	0.3% Max.
Acceptance	0.6 πmm·mrad (normalized)
RFQ linac	
Input/Output energy	8 / 800 keV/u
Vane length	7.3 m
Cavity diameter	0.59 m
Max. surface field	205 kV/cm (1.8 Kilpatrick)
Peak rf power	260 kW (70% Q)
Alvarez linac	
Input/Output energy	0.8 / 6.0 MeV/u
Total length	24 m (3 rf cavities)
Cavity diameter	2.20 / 2.18 / 2.16 m
Average axial field	1.8 / 2.1 / 2.1 MV/m
Shunt impedance	31 – 46 MΩ/m (effective)
Max. surface field	130 kV/cm (1.1 Kilpatrick)
Peak rf power	1.09 / 1.01 / 0.95 MW (80% Q)
Focusing sequence	FODO (6.0 kG/cm Max.)
Output beam emittance	≤ 1.5 πmm·mrad (normalized)
Momentum spread	$\leq \pm 1 \times 10^{-3}$

A phase spread of the accelerated beam is estimated to be 20 deg at the output end of the RFQ, and will be increased to 70 deg during the travel along the LLBT due to a large momentum spread of the beam. A calculation with PARMILA shows that a transmission efficiency through the DTL is not seriously affected by the wide phase spread even for the beam having three times larger longitudinal emittance than an ideally calculated value at the RFQ output. The longitudinal emittance growth in the LLBT, however, tends to introduce an unwanted momentum spread at the output end of the DTL. An input value of a macroscopic longitudinal emittance increases from 5.5 to 18 mrad·MeV/u by a factor of 3.3 after acceleration with the DTL. This situation is shown in Fig. 1, where the longitudinal phase diagrams at the RFQ and DTL outputs are given. A buncher cavity might be required in this line in order to improve the beam characteristics.
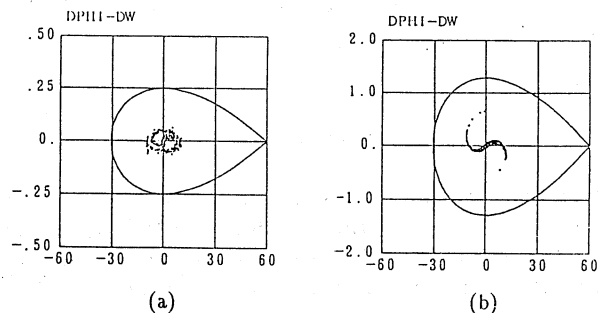

Fig. 1: Examples of the longitudinal phase diagrams at the (a) RFQ and (b) the DTL outputs. The longitudinal emittance increases from 5.5 to 18 mrad·MeV/u mainly by traveling a 1.9 m long LLBT line. The vertical axis indicates the energy difference from the synchronous energy (MeV per unit charge), and the horizontal axis is the phase difference (deg).
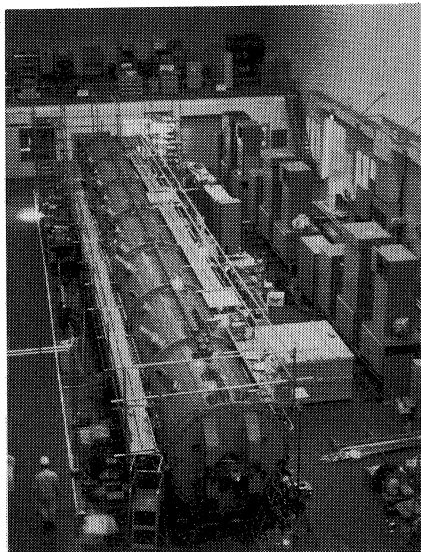
Table 2.
Alvarez linac specification.

	Tank 1	Tank 2	Tank 3
Synchronous phase (deg)	-30	-25	-25
Ion energy (MeV/u)	0.800 – 2.669	2.669 – 4.385	4.385 – 6.060
velocity (%)	4.127 – 7.526	7.526 – 9.634	9.634 – 11.31
Average axial field (MV/m)	1.808	2.102	2.102
Effective shunt impedance* ($M\Omega/m$)	31.5 – 38.7	41.5 – 42.9	45.2 – 45.6
Transit time factor	0.825 – 0.853	0.869 – 0.867	0.888 – 0.880
Quality factor of cavity*	132,000	141,000	143,000
Tank length (m)	9.768	7.202	6.907
Acceleration rate (MeV/m)	1.34	1.67	1.70
Tank diameter (m)	2.20	2.18	2.16
Drift tube diameter (cm)	16.0	16.0	16.0
Drift tube length (cm)	9.85 – 16.45	17.99 – 21.72	22.90 – 25.73
Bore radius (cm)	1.0	1.5	1.5
Nose corner radius (mm)	20	30	30
Corner radius (mm)	10	10	10
Unit cell length (cm)	12.45 – 22.47	22.67 – 28.77	28.99 – 33.79
Gap to cell length ratio	0.214 – 0.265	0.210 – 0.242	0.213 – 0.236
Number of unit cells	56	28	22
Stem radius (cm)	5 and 3	5 and 3	5 and 3
Shunt impedance* ($M\Omega/m$)	46.29 – 53.16	54.93 – 57.07	57.38 – 58.92
Required rf power* (kW)	870	810	760
Q-magnet sequence	FODO	FODO	FODO
Q-magnet length (cm)	6.0, 8.0	12.0	15.0
Field gradient (kG/cm)	6.0, 4.5	3.0	2.4
Phase advance (deg)	42	49	49
Acceptance (πmm·mrad)	67	—	—
Normalized acceptance (πmm·mrad)	2.8	—	—

* Superfish value including stem losses.

Fig. 2: An overview of the Alvarez type linac assembled and tested at Niihama Work, Sumitomo Heavy Industries, LTD. Three sets of the high power amplifiers can be seen at the right of the tank.

Beam dynamic considerations about the DTL

A DTL tank is separated into three independent rf cavities so that an rf power required by each cavity dose not become too high. A diameter of each cavity is about 2 m and changed with one cavity to the next to obtain reasonable values for the transit time factors. A gap to cell length ratio takes a value around 0.22. The maximum surface field is chosen to be 128 kV/cm (1.13 Kilpatrick), resulting an average axial field of about 2 MV/m. The major parameters of the Alvarez linac are listed in Table 2.

Since the transverse emittance of the beam from the RFQ is thoroughly small, a FODO type focusing structure is adopted for a Q-magnet sequence in the drift tubes. The acceptances for FFDD, FODO and FOODOO type focusing sequences are nearly equal if a focusing strength is suitably adjusted. The alignment errors of the Q-magnets, however, affects most seriously for FOODOO structure, because the focusing strength is the strongest for this case.

The 53 quadrupole magnets in the drift tubes are standardized with four different groups: lengths of the magnets are 60, 80, 120 and 150 mm, and field strengths are 6.0, 4.5, 3.0 and 2.4 kG/cm, respectively. The 47 independent power supplies are prepared for these magnets which are operated in a pulse mode with a flat-top-duty of 0.3%. An amplitude of vibration of a drift tube, which is caused by a rapid change in the magnetic field of the Q-magnet, is negligibly small because of the FODO focusing sequence.

The allowable alignment errors for the Q-magnets in the drift tubes are estimated with PARMILA program. The transverse emittance growth is not so serious when the alignment error is $\leq \pm 0.1$ mm in the transverse direction together with the rotation error of $\pm 1°$, the tilt error of $\pm 1°$, and the excitation error of $\pm 0.5\%$. The ellipse parameters in the transverse phase diagram of the accelerated beam are almost kept constant against the error. The center of the ellipse, however, moves around the origin and needs a set of steering magnets in the MEBT line to be matched with the optical axis.

The calculations are also made with the errors in the acceleration field including the field tilt and the phase errors. The phase differences between three tanks affects strongly on the output beam quality when they are $\geq \pm 3°$. The effects of the field tilt, however, are not serious even when the tilt is as high as 10%. An automatic phase controlling system, therefore, is developed to keep the error within $\pm 1°$ with respect to the master oscillator. High power tests using the third DTL cavity show that the system works very stably as expected.[5]

A case study for the trouble of a Q-magnet has been done. The transmission efficiency through the linac decreases to 46% when one of the Q-magnets shuts down. An output phase diagram also changes appreciably. The re-tuning of two adjacent Q-magnets (including the change of the polarity), however, very well recovers the beam characteristics if the input beam is properly adjusted. These processes are indicated in Fig. 3.

Debuncher

A 100 MHz debuncher cavity is introduced in the output beam line to suppress the momentum spread of the accelerated beam. The small momentum spread is very much desired to reduce an rf voltage of an acceleration cavity in a synchrotron ring.

A distance between the DTL end and the debuncher cavity has been optimized to be about 9 m. A phase spread at the debuncher position is broadened to about $\pm 50°$ after the long travel along the MEBT line. An rf voltage of 300 kV (for $q/A = 1/4$) rotates the beam bunch in a longitudinal phase space, and reduces the energy spread of the linac beam from $\Delta W/W = \pm 1.2\%$ to a satisfactorily good value of $\pm 0.11\%$. Some kind of tuning error of the Alvarez linac, however, tends to increase the energy spread up to more than $\pm 0.2\%$. An error of relative phases in the acceleration fields among DTL tanks affects most seriously on the energy spread. Examples of the phase diagrams before and after debuncher cavity are shown in Fig. 4.

Status of the Construction

The beam tests of the PIG source are finished with satisfactory results.[6] The requirements for the beam intensities are fully met for all ion species with a pulsed operation mode. The emittance parameters of the ion beam are measured at the ion source output and used as the initial parameters of the optics calculations for the LEBT line.

The ECR source is now in a stage of the beam tests under the collaboration with the INS, University of Tokyo, and with the RNLR, Tokyo Institute of Technology.[7] The preliminary results show excellent intensities for gaseous ions. The tests of the long term stability and the pulsed operation are going to be done.

Mechanical construction of an RFQ, a DTL and a debuncher cavities are already finished and rf measurements are now under way. The high power tests with third DTL and the debuncher cavities show the excellent performance of these cavities. The parallel operation tests of three DTL cavities are scheduled in this year at Niihama Work of Sumitomo Heavy Industries, LTD. A photograph of the DTL tanks is shown in Fig. 2. In the figure, three sets of the high power amplifiers are seen at the right hand side of the DTL.

The major part of the control system is also completed including a software of a man-machine interface. The combined tests with the real peripheral devices will begin soon at SHI.
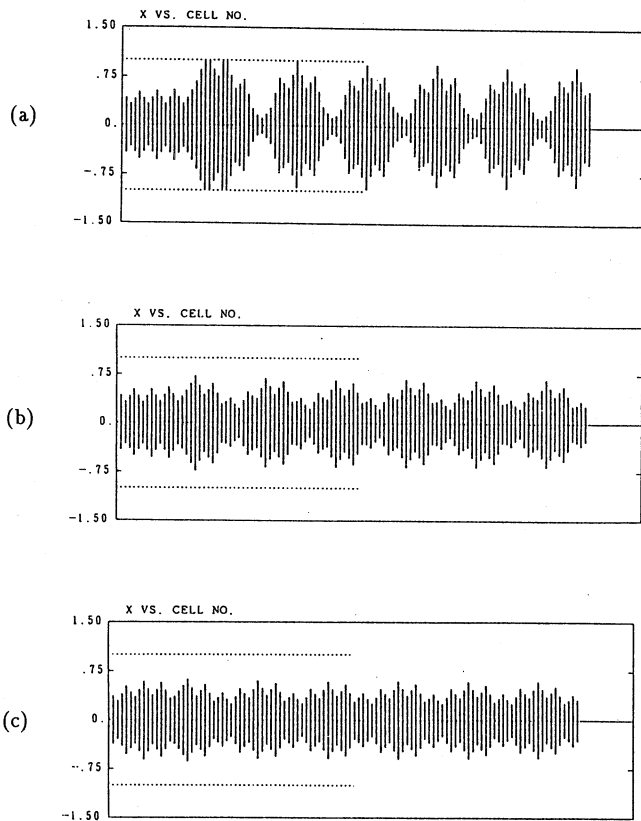
Fig. 3: A case study for a trouble of Q-magnet. (a) No. 16 Q-magnet is set to zero. (b) After tuning of the No. 14 and 18 Q-magnet. (c) After optimization of the input beam. Note that Q-magnet is installed in every second drift tube.

All components will be carried into NIRS during the first 1/4 of 1991. The first beam from the injector will be obtained in 1992.

Acknowledgments

References

(1) Y. Hirao, *et al*, Proc. EPAC90, Nice, France, 1990, p280.

(2) S. Yamada, *et al*, Proc. 6th Symp. Accel. Sci. & Technol., RCNP, Osaka, Japan, 1989, p45.

(3) S. Yamada, *et al*, Proc. 1990 Linac Conf., Albuquerque, New Mexico, USA, 1990, p593.

(4) N. Ueda, *et al*, Proc. 6th Symp. Accel. Sci. & Technol., RCNP, Osaka, Japan, 1989, p59.

(5) K. Sawada, *et al*, this symposium.

(6) Y. Sato, *et al*, Rev. Sci. Instrum. **61**(1), 466 (1990).

(7) A. Kitagawa, *at al*, this symposium.
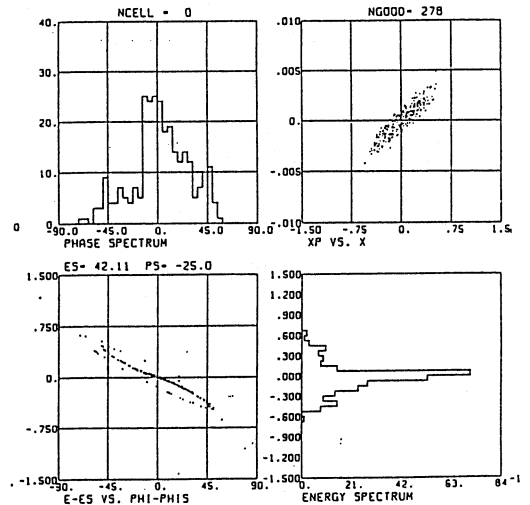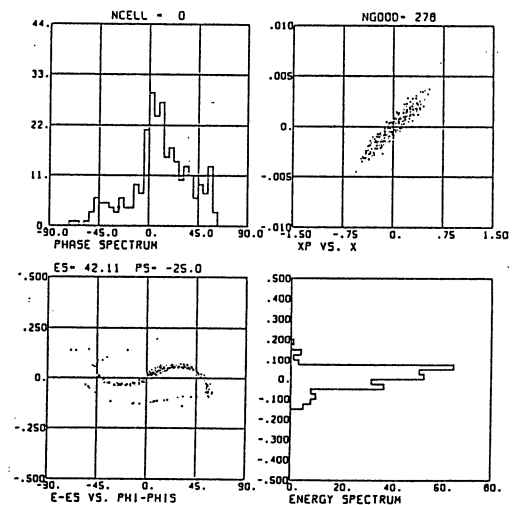
Fig. 4: Examples of the longitudinal phase diagrams and their projections (a) before the debuncher, (b) after the debuncher with a relative phase error of ±1° in DTL cavities.